Received: 21 September 2022 | Revised: 8 February 2023 | Accepted: 3 March 2023

DOI: 10.1002/jemt.24318

REVIEW ARTICLE

MICROSCOPY RESEARCH & TECHNIQUE WILEY

The determination of optimum segmentation parameters using genetic algorithms: Application to different segmentation algorithms and transmission electron microscopy tomography reconstructed volumes

Roberto Fernandez Martinez[1] | Ana Okariz[2] | Maider Iturrondobeitia[3] | Julen Ibarretxe[2]

[1]Department of Electrical Engineering, College of Engineering in Bilbao, University of the Basque Country UPV/EHU, Bilbao, Spain

[2]Department of Applied Physics, College of Engineering in Bilbao, University of the Basque Country UPV/EHU, Bilbao, Spain

[3]Graphic Design and Project Engineering Department, College of Engineering in Bilbao, University of the Basque Country UPV/EHU, Bilbao, Spain

Correspondence
Roberto Fernandez Martinez, Department of Electrical Engineering, College of Engineering in Bilbao, University of the Basque Country UPV/EHU, Alameda Urquijo s/n, Bilbao 48013, Spain.
Email: roberto.fernandezm@ehu.es

Funding information
Basque Government, Grant/Award Number: KK-2019-00033-METALCRO2; University of California, Grant/Award Number: NIGMS P41-GM103311

Review Editor: Alberto Diaspro

Abstract

A method for optimizing an automatic selection of values for parameters that feed segmentation algorithms is proposed. Evolutionary optimization techniques in combination with a fitness function based on a mutual information parameter have been used to find the optimal parameter values of region growing, fuzzy c-means and graph cut segmentation algorithms. To validate the method, the segmentation of two transmission electron microscopy tomography reconstructed volumes of a carbon black-reinforced rubber and a polylactic acid and clay nanocomposite is carried out (i) using evolutionary optimization techniques and (ii) manually by experts. The results confirm that the use of evolutionary optimization techniques, such as genetic algorithms, reduces the computational operation cost needed for a total grid search of segmentation parameters, reducing the probability of reaching a false optimum, and improving the segmentation quality.

Highlights

- A new approach to optimize 3D segmentation algorithms.
- Methodology to optimize segmentation parameters and improve segmentation quality.
- Improvement on the results when using region growing, fuzzy c-means and graph cuts algorithms.

KEYWORDS
characterization, genetic algorithms, microscopy, mutual information, optimization techniques, segmentation, segmentation algorithms, TEM tomography

INTRODUCTION

Quantitative microscopy characterization of material or biological samples requires the segmentation of images (in 2D) or stacks of images (in 3D). Usually, the quality and contrast in the images is frequently poor, making it difficult to define the limits of an object, even for an expert. For this reason, manual segmentations in most cases are time-consuming and subjective. These problems worsen in

transmission electron microscopy (TEM) tomographic reconstructions (Frank, 2006), where the reconstruction process of the sample volume creates artifacts that blur the images and change some of the dimensions of the object, making it difficult to differentiate the object from the background, even for an expert (Midgley et al., 2007; Volkmann, 2010).

Due to this problem, image segmentation topic has been studied over the last few years in different fields. Several algorithms have been implemented to perform segmentation tasks in 2D images collected within the area of artificial vision (Adams & Bischof, 1994; Bezdek et al., 1993; Boykov et al., 2001). This area includes the segmentation of 2D microscopy images, showing how in these images the lack of sharpness of the acquired images complicates the segmentation task. Different specific solutions for each type of characterization problem have been proposed for different microscopy techniques (Kan, 2017; Magliaro et al., 2019; Salahuddin & Qidwai, 2020) and specifically for TEM micrographs (Cao et al., 2019; Groom et al., 2018; Kotrbová et al., 2019).

Semiautomatic segmentation try to overcome these problems, and during the last few years, several solutions have been proposed in this sense. However in this type of segmentation, the process must be guided by the user in several stages, and although quite accurate results have been obtained, the process depends considerably on the user subjectivity (Masubuchi et al., 2020; Mirzaei & Rafsanjani, 2017; Oktay & Gurses, 2019). Semiautomatic segmentation algorithms usually require the selection of the value of one or more parameters that feed the algorithm. Segmentation results for the same algorithm and the image or stack of images can be much more precise if the optimal parameter values are selected. However, the suitable parameter value in every image or stack is not always evident or easy to determine.

Due to the inherent problems of the TEM tomographic reconstruction technique mentioned above (low contrast, blurred images, and artifacts) the intervention of an expert in the semiautomatic segmentation process of this type of 3D image stacks gains more weight and complexity. At the same time some other problems appear. Checking all the possible parameter values to apply in the algorithm by an expert is not affordable due to the high time interval of this process. The number of possible options to evaluate in the case of 3D image stacks is greatly increased compared a 2D image. The problem is intensified even more when advanced algorithms are applied since the computational cost increases considerably. And performing a comparison of segmentation results, usually based on a visual inspection, after using different parameter values become a complex task and sometimes difficult to evaluate. In the case of some algorithms, specific methods have been proposed that make it possible to determine a suitable range of values or even a specific value of the parameters that optimizes the result (Jing et al., 2014; Peng & Veksler, 2008; Yu et al., 2004), though this is not always the case.

When the semiautomatic segmentation process is not performed optimally, it is difficult to achieve a reliable quantitative result or to compare results between different algorithms to choose the most suitable one for each kind of image or image stack. The aim of this work is to find a general methodology to overcome these problems, that is, a methodology to perform the optimal segmentation determining the optimal parameter values of any segmentation algorithm within a reasonable time interval.

The classical selection of the optimal values of these segmentation parameters frequently fails since the segmentation process has many local optimums. To overcome these issues, there is a need to extend further powerful optimization techniques to obtain the global optimum (Aslam & Santhi, 2020). One of the most widely used optimization techniques is evolutionary optimization, since they usually calculate an optimal solution in problems with multiple solutions, assigning a fitness value to each solution, forming a ranking and generating a solution with a high probability of being around the correct solutions in the population (Simon, 2013). These techniques have been applied in several engineering applications to solve similar problems (António & Hoffbauer, 2017; Lostado et al., 2012; Sanz-García et al., 2012; Xiao et al., 2020). As well as in problems related to image processing but far from the cases under study in this work, 3D TEM tomographic reconstruction (Abdel-Khalek et al., 2017; Elaziz & Lu, 2019; Hilali-Jaghdam et al., 2020).

In this work, these techniques have been used to determine the optimal parameter values for three segmentation algorithms that have been used to segment two stacks of images obtained by the TEM tomography technique. The use of optimization techniques is considered necessary to work with stacks of images of considerable size, since achieving the optimal parameter values for the most accurate segmentation by performing a grid search through all points of the stack can be immeasurable in terms of time consumption and computational cost. The proposed evolutionary optimization is based on genetic algorithm (GA) techniques. The parameters that define the segmentation process of each segmentation algorithm are utilized to form the chromosome. These chromosomes define each individual of each generation. The quality of each individual is evaluated through a fitness function. The process is mainly focused on the mutation and the crossover between individuals of different generations, where only the individuals who obtain accurate segmentations can be part of the next generation, while getting new generations that improve results generation by generation (Simon, 2013). The selection of individuals of this evolutionary methodology is based on a fitness function that provides the value of a mutual information coefficient, MI (Okariz et al., 2017). The segmentations with higher values of MI are the segmentations with higher accuracies and, consequently, define the individuals for the following generation.

And finally, in order to measure the computational cost that allows analyzing the time interval necessary to achieve an optimal segmentation, three techniques to select optimal segmentations are compared: analysis of all possible combinations of each algorithm (grid search), the search for the optimal values using GA (GA-based), and search for the optimum by a semimanual segmentation (manual segmentation).

Summarizing, the main idea of this work is to verify following the proposed methodology (i) that the optimum values of segmentation parameters of any algorithm can be obtained in an automatic way improving the segmentation quality; (ii) that the time interval in

comparison with the one required to check the whole space of possibilities can be reduced; and (iii) that the results obtained improve the quality of those obtained by experts using the same algorithm.

The results show that the GA-based optimization achieves the best computational cost and segmentation accuracy ratio. The computational cost needed to find the optimal value is considerably reduced in comparison with the cost needed to evaluate all possible combinations according to the grid search process. In addition, the segmentation quality improves the manual segmentation results.

1 | MATERIALS AND METHODS

The most accurate segmentation defined by the optimum parameter values of three segmentation algorithms for two different stacks of images was performed by evolutionary optimization based on GA techniques, as well as manually by experts. To evaluate the results, (i) the time needed to perform the segmentation and (ii) the segmentation quality is measured. This methodology is described in detail below.

1.1 | Stacks of images

The methodology proposed in this work has been evaluated in two image stacks corresponding to the following TEM tomographic reconstructions:

- Stack 1: a stack of gray images of a carbon black (CB) (N330)-reinforced EPDM rubber. The stack dimensions are 182 × 164 × 182 px. The sample (10 phr of CB) was prepared in an internal mixer and a cryo-microtome into 120 nm thick slices. The TEM tomography reconstruction and some orthoslices are shown in Figure 1. The Fiji package (Rueden et al., 2017; Schindelin et al., 2012) was used to visualize the orthoslices. The reconstruction was calculated from images acquired in a TEM operated in bright field mode (BF-TEM) with TOMO3D software (Agulleiro & Fernandez, 2011). The tilted images were acquired from −60° to 60° every 1° in an FEI Tecnai G2 20 TWIN microscope at 200 kV, with a pixel size of 0.91 nm.
- Stack 2: a stack of gray images of a polylactic acid (PLA)/clay nanocomposite (details about the sample in Iturrondobeitia et al., 2017) for TEM tomography reconstruction (Figure 2) calculated from images acquired in TEM operated in BF-TEM mode with Inspect 3D software and the SIRT algorithm (five iterations). The stack dimensions are 169 × 268 × 137 px. The tilted images were acquired from −70° to 70° every 2° in a Zeiss EM 912 Omega microscope at 120 kV, with a pixel size of 1.1 nm.

1.2 | Segmentation algorithms

The stacks of images have been segmented with three segmentation algorithms implemented in MATLAB scripts (MATLAB, 2020): region growing (RG) (Adams & Bischof, 1994), fuzzy c-means (FCM) (Bezdek et al., 1984), and graph cuts (GC) (Boykov et al., 2001).

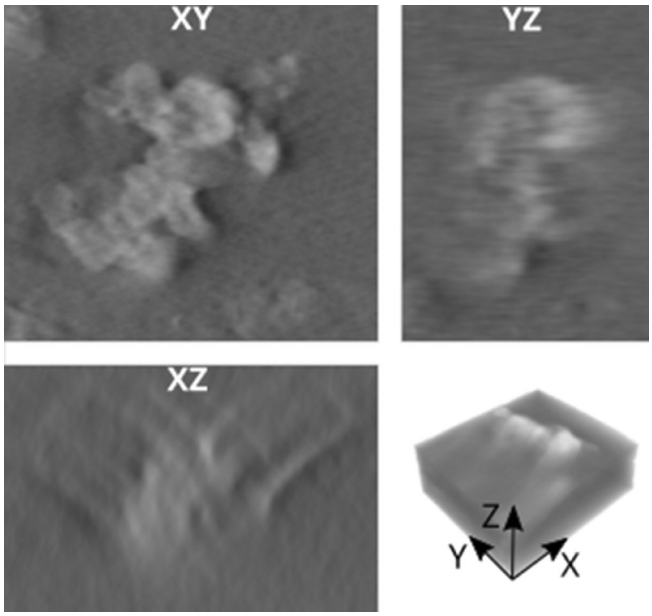

FIGURE 1 TEM tomography reconstruction of a CB(N330)-reinforced EPDM rubber (sample 1). The stack of the tomography reconstruction and the orthoslices indicated in the volume are shown.

1.2.1 | Region growing

This is a clustering-based algorithm. Clustering is a process where objects are classified in such a way that items in the same cluster are as similar as possible, while items belonging to different clusters are as dissimilar as possible. The RG algorithm examines neighboring pixels of a selected initial seed point and determines whether the pixel neighbors should be added to the region to which the seed belongs according to similarity constraints (Adams & Bischof, 1994). The process is iterative, and it is continued until all pixels belong to a region.

Each step of the algorithm involves the addition of one pixel to one of the $A_1, A_2, \ldots, A_n$ sets defined for image segmentation. Let $N(x)$ be the set of immediate neighbors of pixel x. If we assume that $N(x)$ meets just one of the A_i, then we define $i(x) \in \{1,2,\ldots n\}$ to be that index such that $N(x) \cap A_i(x) \neq \varnothing$ and define $\delta(x)$ to be a measure of how different x is from the region it adjoins. The simplest definition for $\delta(x)$ is $\delta(x) = |g(x) - \text{mean}_{y \in A_{i(x)}}[g(y)]|$, where $g(x)$ is the gray value of the image point x. If $N(x)$ meets two or more of the A_i, $i(x)$ is taken to be a value of i such that $N(x)$ meets A and $\delta(x)$ is minimized. The pixel with the smallest difference measured this way is allocated to the region.

The suitable selection of seed points is a decisive factor in the quality of the segmentation. In the algorithm implementation that has been used in this work (Daniel, 2021), another two parameters must be chosen: the maximum distance to the initial position and the absolute threshold level to be included in the segmentation. The

optimization of the segmentation results for this algorithm requires the appropriate selection of these three values (the coordinates of a seed point, the maximum distance to the initial position and the threshold) (Table 1). The range of these parameters must be delimited to make the selection process of their optimum value possible by using the method proposed in this work. All the pixels of the image are eligible as seed points, and the threshold value range is the image gray value range, that is, [0,250]. The maximum distance has been estimated as the largest dimension of the object to be segmented in all cases.

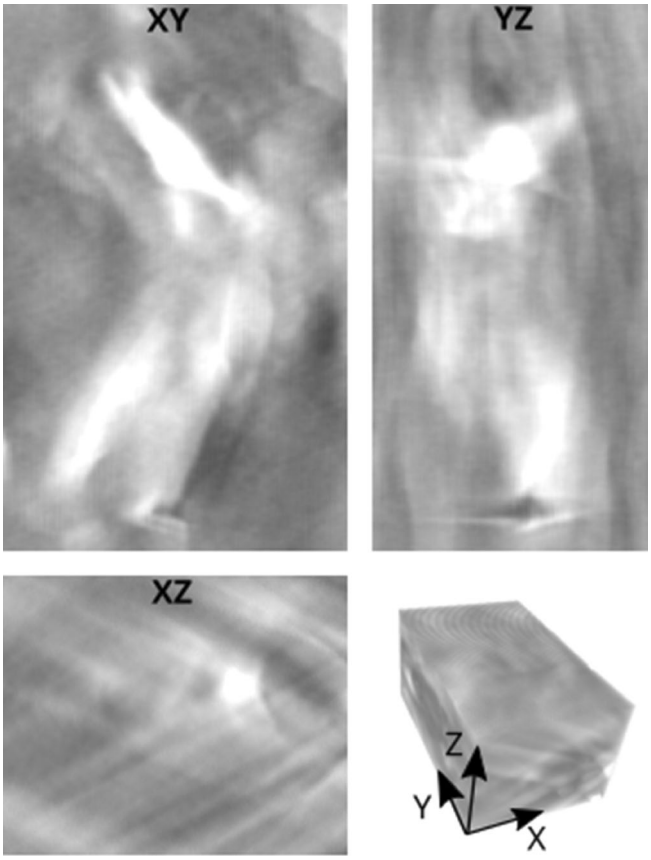

FIGURE 2 TEM tomography reconstruction of a PLA/clay nanocomposite (sample 2). The stack of the tomography reconstruction and the orthoslices indicated in the volume are shown.

1.2.2 | Fuzzy c-means

The FCM algorithm is another clustering-based algorithm. In fuzzy clustering, data points can potentially belong to multiple clusters, and membership grades are assigned to each of the data points (tags). Among the fuzzy clustering methods, the FCM algorithm is the most popular method used in image segmentation because it has robust characteristics for ambiguity (Bezdek et al., 1993).

This iterative clustering method produces an optimal c partition of the image in different regions by minimizing the weighted within-group sum of the squared error objective function J_{FCM} (Equation 1) (Bezdek et al., 1984).

$$J_{FCM} = \sum_{k=1}^{n} \sum_{i=1}^{c} (u_{ik})^2 d^2(x_k, v_i), \quad (1)$$

where u_{ik} is calculated as shown in Equation (2).

$$u_{ik} = \frac{1}{\sum_{j=1}^{c} \left(\frac{d_{ik}}{d_{jk}}\right)^{\frac{2}{(q-1)}}}, \quad (2)$$

where $X = \{x_1, x_2, ..., x_n, \} \subseteq R^P$ is the dataset in the p-dimensional vector space, n is the number of data items, c is the number of clusters with $2 \le c < n$, u_{ik} is the degree of membership of x_k in the ith cluster, q is a weighting exponent on each fuzzy membership, v_i is the prototype of the centre (the mean of all points, weighted by their degree of belonging to the cluster) of cluster i, d_{ik} is the Euclidean distance between x_k and v_i, and $d^2(x_k, v_i)$ is a distance measurement between object x_k and cluster centre v_i.

In this work, the c number of clusters is two (object and background), and the q weighting exponent on each fuzzy membership must be adjusted to find the best segmentation result. This weighting exponent is a parameter that greatly influences the performance of the algorithm, and some rules and algorithms have been proposed for selecting it (Jing et al., 2014; Okeke & Karnieli, 2006; Yu et al., 2004) (Table 1). The application of these rules and methods allows obtaining a possible range of values for the exponent, but not with a specific value. In the algorithm implementation that has been used (Semechko, 2021), this weighting exponent has to be a minimum value of 1.1.

TABLE 1 Summary of the parameters that feed the segmentation algorithms.

Segmentation algorithm	Parameter	Brief definition
Region Growing (RG)	Seed	Coordinates of an initial point of the object
	Threshold value	Absolute threshold level to be included in the segmentation
	Distance	Maximum distance to the seed
Fuzzy c-Means (FCM)	Weighting exponent	Weighting exponent on each fuzzy membership
Graph Cuts (GC)	Smoothing weight	Smoothing factor of the boundaries between the object and background
	Threshold value	Absolute threshold level to be included in the segmentation

Note: Detailed information about the characteristics of the algorithms can be found in Adams and Bischof (1994) for RG, Bezdek et al. (1984) for FCM, and Boykov and Kolmogorov (2004) for GC.

1.2.3 | Graph cuts

The GC algorithm is a combinatorial graph theory algorithm (Boykov et al., 2001). Each pixel in an image is considered a node in a graph and added to two terminal nodes connected to every pixel, named S (source) and T (sink). Each of these two nodes would be associated with an object or a background label. Once the graph is built, the labelling of the pixels is carried out through a cut on the graph. This cut will sever two types of links:

- t-links: a cut removes one of the two edges that connects a pixel with a terminal S or T node, associating it this way to the object or background class.
- n-links: a cut removes the links between pairs of pixels associated with different terminals.

Boykov and Jolly (2001) defined the cut among all the possible solutions using the max-flow min-cut theorem, which was originally formulated on a flow network. This type of graph models a flow distribution network from a source S to a sink T, where each edge is labeled with a certain capacity. In the context of the GC, these capacities are called weights or costs. The cost of n-links is determined by a function that only penalizes neighboring pixels assigned to different labels, which take large values when those pixels are similar. The cost of t-links is usually associated with a penalty that reflects how the pixel intensity fits into an estimated model of the object or background. The flow that circulates through this network must satisfy two constraints:

- Each edge in the graph has an associated capacity (cost) that limits the maximum flow that can circulate through it.
- The sum of the flow entering a node must correspond to the sum of the exit flow.

The weighting of the graph edges allows the definition of a cost function $E(A)$ that combines the defined weights given a certain labelling of the pixels and is represented by a binary vector A. We consider an arbitrary set of data elements P and some neighborhood system represented by a set N of all unordered pairs $\{p,q\}$ of neighboring elements in P. The constraints imposed on the boundary and the region properties of A are described by the cost function $E(A)$ (Equation 3) as follows:

$$E(A) = \lambda R(A) + B(A), \tag{3}$$

where

$$\begin{aligned} R(A) &= \sum_{p \epsilon P} R_p(A_p) \\ B(A) &= \sum_{\{p,q\} \epsilon N} B_{\{p,q\}} \cdot \delta(A_p, A_q) \end{aligned} \tag{4}$$

and

$$\delta(A_p, A_q) = \{1\, 0 \, if \, A_p \neq A_q \, \text{otherwise}. \tag{5}$$

The coefficient λ specifies the relative importance of the region properties term $R(A)$ versus the boundary properties term $B(A)$. Coefficient $B_{\{p,q\}}$ should be interpreted as a penalty for a discontinuity between p and q. The minimisation of this $E(A)$ cost function corresponds to the resulting labelling of the min-cut on the graph.

A MATLAB script is developed to implement this algorithm. In this implementation two parameters must be adjusted: (a) a threshold value to be included in the segmentation and (b) the smoothness degree of the boundaries between the segmented regions (smoothing weight) (Table 1). The gray range of the image stack ([0,250]) has been considered the range of the threshold values with a [0,15] range for the smoothing weight.

1.3 | Automatic segmentation: Optimization using genetic algorithms

GA combined with the studied segmentation algorithms are selected to obtain the optimum segmentation of 3D stacks of images. The main idea of the GA is biological evolution. By applying replication, crossover, mutation and selection, the next generations of the population are generated, evolving to solve the problem. This evolution is defined by a fitness function (MI) that is used to eliminate individuals with lower environmental adaptability to obtain the most suitable offspring.

In this case, the parameters that define each individual are the parameters that define each of the segmentation algorithms. The values and the ranges of these parameters are obtained according to the operation process of each segmentation algorithm, and they determine the starting point of the optimization process. This process is performed in six stages: population initialization, encoding/decoding, evaluation, selection, crossover and mutation. A flow chart showing how these six steps explain the GA methodology can be seen in Figure 3. The specific steps that define the GA process are as follows.

- Population initialization: To generate an initial population with individuals formed by different properties, a random initialization of each parameter value is performed to define the segmentation algorithms, and subsequently, the individuals.
- Encoding/decoding: Each individual of the population is defined by some characteristic information, in this case, the value of the main parameters that define the segmentation algorithms. During the encoding stage, this information is transformed into binary code forming the chromosome that defines each individual (Figure 4). During the decoding, the binary information of the chromosome is transformed to obtain the information of the parameters that define the segmentation algorithms. During these two stages, the process is limited to values that are defined within the operating range of the parameters of each segmentation algorithm.
- Evaluation: The segmentation algorithms, defined with a proper parameter setting, must be evaluated using a fitness function. This process determines which individuals of the studied generation

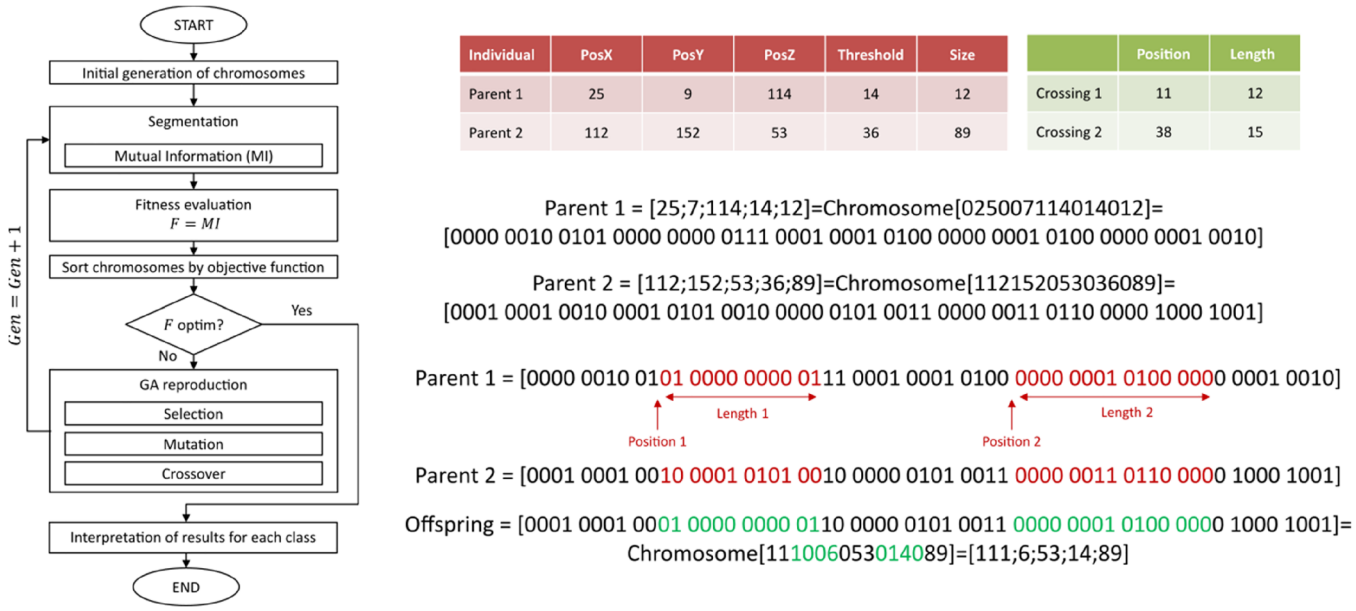

FIGURE 3 Flow chart that follows the GA methodology. Details of the crossover process based on the segmentation algorithm RG.

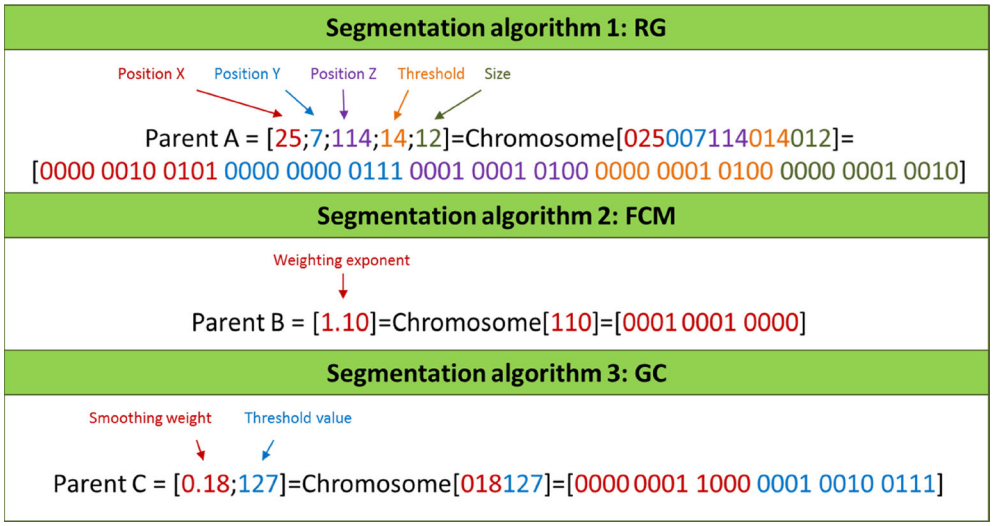

FIGURE 4 Encoding process and generation of chromosomes of an individual in the three segmentation algorithms studied.

provide more precise segmentations, and therefore, it can help to select these elite individuals to be part of the next generation. In this case, the fitness function to evaluate the solution domain is defined by the MI function (see Section 2.5), which allows evaluating the quality of the performed segmentation.

- Selection: The individuals of the current generation who have performed more accurately when evaluated by the fitness function are selected to form the next population of possible solutions to the problem. In this case, it was defined that 25% of individuals of the next generation come from this selection process.
- Crossover: Recombination between chromosomes of two of the parents that are part of the current generation allows the creation of the new offspring. The portion of the chromosome that is taken from each of the parents is defined by a random selection. This selection is defined according to two positions and two lengths, which select a random number of bits of the chromosomes of the chosen parents to obtain offspring of future generations (Figure 3). This selection makes it possible to create new offspring with part of the chromosomes from both parents. In this case, it was defined that 25% of individuals of the next generation come from this crossover process.
- Mutation: The goal of applying mutations in this evolutionary process is to generate diversity among the individuals of the population. In this way, convergence in local minima is avoided. This process selects a number of random bits at random positions on the chromosome, flipping the value of the selected bits. In this case, it was defined that 50% of individuals of the next generation come from this mutation process. These mutations are performed from 25% of the selected individuals and from 25% of the crossover individuals.

Furthermore, during the process when any of the variables that form the chromosome of new offspring are outside of the range of admissible values, these offspring are removed from the population, and the process is repeated until a complete generation is generated.

This automatic process is used for the optimization of the segmentation of the two image stacks defined in Section 2.1. In both cases, the population size per generation is set to 100 individuals for the FCM and GC algorithms and 200 individuals for RG. The first generation is completely random, and the following generations maintain the same population for each case. During the methodology adjustment, the number of generations necessary to converge to a solution is analyzed, finding the global optimum in each case. Initial tests are carried out to evaluate the ratio between the improvement of the MI coefficient and the computational cost of the process, concluding that the number of generations to be used is 25 for the RG algorithm, 5 for the FCM algorithm and 15 for the GC algorithm.

1.4 | Manual segmentation

Manual segmentation depends on many factors: the software, the methodology for selecting the parameters, the criteria for selecting the final segmentation, and so forth. In addition, experts do not usually perform real manual segmentation; iterative or repetitive tasks are usually performed semi-automatically using specific programs designed for these tasks. In this work, a semiautomatic segmentation process has been employed, that is, a process that resembles the user's workflow in the segmentation operation and that only requires the user's intervention to choose the initial set of parameter values to test the segmentation algorithm. A specific script implemented in MATLAB asks for these values, checks the segmentation results for these parameters, refines the search for their optimal value and provides the final segmentation result in the same way as the user would.

The methodology for selecting the parameters is as follows: the user selects a series of n initial values for the parameters $s_1, s_2, \ldots, s_n$, and the corresponding n segmentations are calculated. The segmentation quality is evaluated using the same fitness function, MI. The s_i segmentation parameter or set of parameters with the highest value of the fitness function are then selected, and the search is refined in the $[s_i, s_{i+1}]$ interval. This refining process is carried out by calculating the segmentations corresponding to $s_{i-1}+\Delta s, s_{i-1}+2\Delta s, \ldots, s_{i+1}-2\Delta s, s_{i+1}-\Delta s$ values, where $\Delta s = \frac{s_{i+1}-s_i}{3}$. In case the same maximum is obtained for several parameter values, the refining process is carried out in all the intervals centered on each of them. The initial seed coordinates of the RG algorithm are the exception to this issue, which remain unchanged. The quality of the segmentations is again evaluated, and the process is repeated iteratively until the value of the fitness function no longer increases. The final segmentation is the segmentation with the highest fitness function value.

In Table 2, the initial parameter values used for the three segmentation algorithms are shown. To select the initial threshold values, the gray value profile is plotted along a straight line across the object. The range of values corresponding to the transition area between the object and the background is used as the threshold range. The initial seeds used in RG are selected by an expert choosing pixels that clearly belong to the object.

1.5 | Time interval and quality measurements

This work is focused on find an adequate ratio between the time required to find the optimal segmentation solution and the precision of this segmentation.

The requested time to find the optimal segmentation parameter values (computational cost) is measured for GA-based optimization and manual segmentation. Since testing all the possible combinations would take too long, in the grid search optimization, this time has been estimated from the mean times obtained during the application of evolutionary computation. All computational cost measurements are measured on the same server.

The segmentation accuracy is evaluated with the MI coefficient. This coefficient has been previously used successfully by Okariz et al. (2017) to segment TEM images. The MI coefficient (Cover & Thomas, 1991; Shannon & Weaver, 1949) calculates the accuracy of a segmentation comparing the original TEM images of a sample and their corresponding Radon projections computed from different segmentations (Equation 6).

$$\mathrm{MI} = \sum_{a,b} P_{AB}(a,b) \log \frac{P_{AB}(a,b)}{P_A(a) P_B(b)}, \tag{6}$$

where $P_A(a)$ and $P_B(b)$ are the normalized marginal histograms of images A and B, respectively $P_{AB}(a,b)$ is their joint histogram, and a and b are the intensity values of a pair of voxels in images A and B (Maes et al., 1997). Higher MI values indicate a larger reduction in uncertainty (high match between images), and a 0 value means the variables (images) are statistically independent.

Both the quality of all the segmentations and the fitness functions for evaluating the GA evolution and the manual segmentation processes have been measured based on this function, which is calculated as follows:

- First, the segmentation of the stack of images of the tomographic reconstruction is carried out with the chosen parameter values for the selected segmentation algorithm.
- Then, the Radon transform of the segmented volume is calculated to simulate the microscope image of the sample.
- Finally, the MI coefficient is calculated between the original TEM image at 0° tilt and this Radon transform.

2 | RESULTS AND DISCUSSION

The validation of the proposed automatic methodology has been based on the segmentation of the two image stacks described in Section 2.1.

Segmentation algorithm	Parameter	Initial values selected by the user	
		Sample 1: CB	Sample 2: PLA
RG	Seed	5 seeds	4 seeds
	Threshold value	75, 100, 125, 150	100, 150, 170, 200
FCM	Weighting exponent	2, 3, 6, 12, 25, 50	
GC	Smoothing weight	0, 0.5, 1, 2, 4, 8, 15	
	Threshold value	75, 100, 125, 150	100, 150, 170, 200

TABLE 2 Initial values of the parameters that feed the segmentation algorithms in the manual segmentation.

Segmentation algorithm	Variable	Lower bound	Upper bound	Increment
RG	Position *X*	1	181	1
	Position *Y*	1	163	1
	Position *Z*	1	181	1
	Threshold value	0	255	1
	Region size	10	100	1
FCM	Weighting exponent	1.1	100	0.1
GC	Smoothing weight	0	15	0.1
	Threshold value	0	255	1

TABLE 3 Segmentation parameters design for stack 1 (CB).

TABLE 4 Time interval to complete the segmentation process and the number of performed segmentations.

Segmentation algorithm	Computational time (minutes)			Number of iterations		
	Grid search (estimation)	GA (measured)	Manual (measured)	Grid search	GA	Manual
RG	728×10^9	28,350	590.35	128×10^9	5,000	41
FCM	227.47	115	0.50	989	500	13
GC	187,042.50	7,335	48.12	38,250	1,500	93

Note: Comparison between the three algorithms in study case 1 (Carbon black).

2.1 | Stack 1: CB(N330)-reinforced EPDM rubber

For the first stack of images, the parameters that define the three segmentation algorithms and their ranges are shown in Table 3. These values must be defined in advance since determine the possible options to perform a segmentation, and also the search space for the optimal segmentation.

As previously mentioned, this search has been analyzed by three ways (Grid search, GA-based, and manual) focused into obtain the optimal segmentation of each of the studied image stack. In Table 4, the computational cost or time interval required to choose the segmentation parameter values that leads to the optimal segmentation as well as the number of cases that have been compared in the process are shown for each algorithm. The results show that two of the optimization methods (manual and GA-based) reduce the computational cost significantly when it is compared with the grid search analysis, particularly in the case of RG algorithm where its application is really time consuming.

It can be concluded, based on the results, that both the number of analyzed cases and the time needed to obtain the optimal segmentation are higher in the automatic evolutionary optimization technique process than in the manual process, although the search is more exhaustive in the first process. In this case, Figure 5 shows that high-precision segmentations are reached based on MI results in a reduced number of generations.

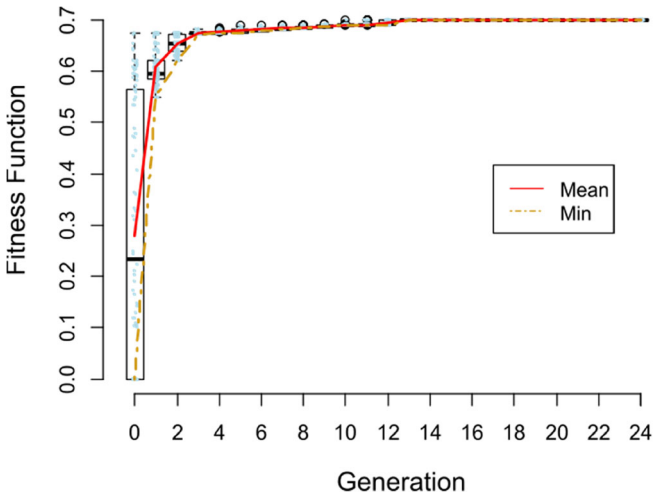

FIGURE 5 Evolution of the objective function (MI) during the GA evolutionary process. Study case 1: Carbon black stack and RG segmentation algorithm.

TABLE 5 Optimal parameters and segmentation quality measurements (MI) for the RG algorithm according to the automatic (GA-based) and manual optimization processes.

	Position *X*	Position *Y*	Position *Z*	Threshold	MI
Manual	117	61	78	150	0.6876
GA	146	149	123	89	0.6997

Note: Study case 1.

TABLE 6 Optimal parameters and segmentation quality measurements (MI) for the FCM algorithm according to the automatic (GA-based) and manual optimization processes.

	Weighting exponent	MI
Manual	2	0.5235
GA	81.9	0.5300

Note: Study case 1.

TABLE 7 Optimal parameters and segmentation quality measurements (MI) for the GC algorithm according to the automatic (GA-based) and manual optimization processes.

	Smoothing weight	Threshold	MI
Manual	0	75	0.3184
GA	0.1	100	0.7150

Note: Study case 1.

Time reduction is not the only important aspect of this process; the accuracy level of segmentation is also studied. Tables 5–7 show the quality results, as well as the optimal parameter values for each segmentation algorithm. The values of the fitness function (MI) are higher for the GA-based optimization method for the three proposed algorithms, especially for the GC algorithm.

In this case, where CB stack of images is analyzed, the GA-based optimization algorithm improves the segmentation accuracy when the three studied algorithms are applied. Moreover the computational cost is not excessively higher in comparison with of the manual optimization, especially when both are compared with the search process based on the grid search analysis.

2.2 | Stack 2: PLA/clay nanocomposite

In a similar way than with the stack of images 1, Table 8 defines the parameters than define the three segmentation algorithms and their ranges. In addition, the same three methods to search for the optimal segmentation are analyzed. Table 9 shows the results for the computational cost and the number of performed segmentations. As in the previous stack, it can be observed that the computational time is considerably reduced in manual and GA-based optimization methods in comparison with the grid search analysis.

TABLE 8 Segmentation parameters design for stack 2 (PLA/clay nanocomposite).

Segmentation algorithm	Variable	Lower bound	Upper bound	Increment
RG	Position *X*	1	154	1
	Position *Y*	1	267	1
	Position *Z*	1	181	1
	Threshold value	0	255	1
	Region size	10	100	1
FCM	Weighting exponent	1.1	100	0.1
GC	Smoothing weight	0	15	0.1
	Threshold value	0	255	1

TABLE 9 Time interval to complete segmentation process and number of segmentations performed.

	Computational time (minutes)			Number of iterations		
Segmentation algorithm	Grid search (estimation)	GA (measured)	Manual (measured)	Grid search	GA	Manual
RG	178×10^9	32,050	9,913.17	1147×10^9	5,000	1,865
FCM	217.58	110	0.49	989	500	13
GC	182,070.00	7140	10.80	38,250	1,500	30

Note: Comparison between the three algorithms in the study case 2 (PLA/clay nanocomposite).

TABLE 10 Optimal parameters and segmentation quality measurements (MI) for the RG algorithm according to the automatic (GA-based) and manual optimization processes.

	Position *X*	Position *Y*	Position *Z*	Threshold	MI
Manual	188	51	60	58	0.6033
GA	94	115	86	44	0.6051

Note: Study case 2.

As in the previous case, the optimal segmentations based on evolutionary techniques obtain higher quality results than the manual segmentations (Tables 10–12), although they require more time for the calculations. Again, the segmentation accuracy is greater for the GA-based optimization method and the three algorithms, especially with the GC algorithm.

TABLE 11 Optimal parameters and segmentation quality measurements (MI) for the FCM algorithm according to the automatic (GA-based) and manual optimization processes.

	Weighting exponent	MI
Manual	2	0.4568
GA	1.5	0.4633

Note: Study case 2.

TABLE 12 Optimal parameters and segmentation quality measurements (MI) for the GC algorithm according to the automatic (GA-based) and manual optimization processes.

	Smoothing weight	Threshold	MI
Manual	0	100	0.0719
GA	2	166	0.7942

Note: Study case 2.

2.3 | Comparison of manual and automatic segmentation methods

According to the previous results, it can be concluded that in both stacks, the computational cost is lower in terms of the manual process for the three algorithms (as was expected, since the number of performed segmentations is lower) and that the segmentation quality is higher in terms of the GA-based segmentation results.

Two examples of the segmentation results are shown in Figures 6 and 7. In Figure 6 (Stack 1: CB(N330)-reinforced EPDM rubber), a substantial improvement is observed since the manual method does not allow us to obtain coherent segmentation, while the GA-based segmentation does obtain more precise segmentation. In Figure 7 (Stack 2: PLA/clay nanocomposite), it is observed that the improvement is not evident from visual inspection, although once again, the segmentation based on generic algorithms improves the manual segmentation according to the MI fitness function.

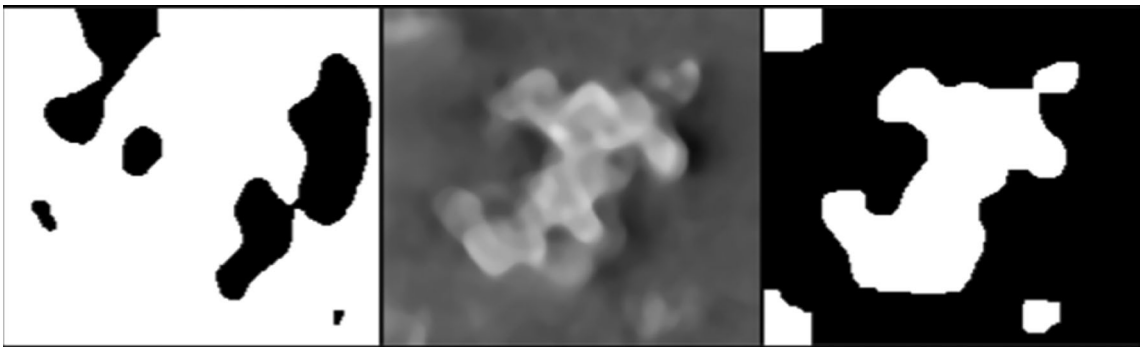

FIGURE 6 Details of the OXY central section of the two GC final segmentations of stack 1. The figure on the left corresponds to the result obtained by manual selection of the segmentation parameters, and the figure on the right corresponds to the result obtained by GA. The central image is the corresponding slice of the TEM tomographic reconstruction.

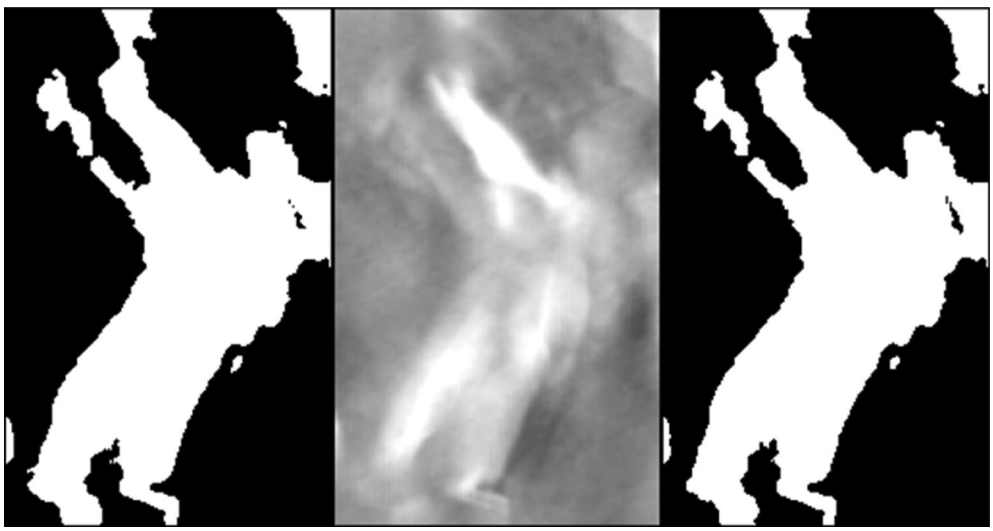

FIGURE 7 Detail of the OXY central section of the two FCM final segmentations of stack 2. The figure on the left corresponds to the result obtained by manual selection of the segmentation parameters, and the figure on the right corresponds to the result obtained by GA. The central image is the corresponding slice of the TEM tomographic reconstruction.

GA-based optimization requires a higher computational cost in comparison with manual optimization. However, this computational cost is acceptable considering (i) that both methods greatly reduce the cost needed to perform a total grid search, especially when using RG and GC segmentation methods, and (ii) that the obtained segmentation accuracy using GA improves manual segmentation in all cases. Consequently, it can be concluded that GA-based optimization generates higher quality segmentations. In addition, this technique can be applied to any other automatic segmentation algorithm to search for the optimum segmentation parameters because it does not depend on the specific algorithm used for segmentation. Only minor adjustments should be made to use with another segmentation algorithm: (i) the number of parameters to be analyzed and (ii) their respective value ranges.

3 | CONCLUSIONS

Evolutionary optimization techniques based on GAs can be used to evaluate segmentation algorithms in a more efficient way than a manual evaluation because a larger number of parameter values can be considered in an affordable time interval. In addition, the results corroborate that the segmentation quality improves using a GA-based optimization of segmentation parameters. These results not only validate the method but also prove that an automatic optimization of segmentation parameter values leads to more accurate segmentations with an affordable computational cost, while avoiding the subjectivity problems of manual segmentation procedures.

AUTHOR CONTRIBUTIONS

Conceptualization, R.F.M. and A.O.; methodology, R.F.M. and A.O.; software, R.F.M. and A.O.; validation, R.F.M., A.O. M.I. and J.I.; formal analysis, R.F.M. and A.O.; investigation, R.F.M., A.O., M.I. and J.I.; resources, R.F.M., A.O., M.I. and J.I.; data curation, A.O, M.I. and J.I.; writing–original draft preparation, R.F.M. and A.O.; writing–review and editing, R.F.M., A.O, M.I. and J.I.; visualization, R.F.M. and A.O.; supervision, R.F.M. and A.O.; project administration, R.F.M., A.O., M.I. and J.I.; funding acquisition, R.F.M., A.O., M.I. and J.I.; All authors have read and agreed to the published version of the manuscript.

ACKNOWLEDGMENTS

The authors would like to thank PhD Saad Ullah Akram for the script of the GC-based segmentation algorithm and the Basque Government for financial support through the KK-2019-00033-METALCRO2 project. The volume representations of the reconstructions were performed with the UCSF Chimera package (Pettersen et al., 2004). Chimera is developed by the Resource for Biocomputing, Visualization, and Informatics at the University of California, United States, San Francisco (supported by NIGMS P41-GM103311).

DATA AVAILABILITY STATEMENT

The data that support the findings of this study are available from the corresponding author upon reasonable request.

ORCID

Roberto Fernandez Martinez https://orcid.org/0000-0002-9436-6577

REFERENCES

Abdel-Khalek, S., Ben Ishak, A., Omer, O. A., & Obada, A. S. F. (2017). A two-dimensional image segmentation method based on genetic algorithm and entropy. *Optik*, *131*, 414–422.

Adams, R., & Bischof, L. (1994). Seeded region growing. *IEEE Transactions on Pattern Analysis and Machine Intelligence*, *16*(6), 641–647.

Agulleiro, J. I., & Fernandez, J. J. (2011). Fast tomographic reconstruction on multicore computers. *Bioinformatics*, *27*(4), 582–583.

António, C. C., & Hoffbauer, L. N. (2017). Reliability-based design optimization and uncertainty quantification for optimal conditions of composite structures with non-linear behavior. *Engineering Structures*, *153*, 479–490.

Aslam, Y., & Santhi, N. (2020). A comprehensive survey on optimization techniques in image processing. *Materials Today: Proceedings*, *24*(3), 1758–1765.

Bezdek, J., Ehrlich, R., & Full, W. (1984). FCM-the fuzzy C-means clustering-algorithm. *Computers & Geosciences*, *10*, 191–203.

Bezdek, J. C., Hall, L. O., & Clarke, L. P. (1993). Review of MR image SegmentationTechniques using pattern recognition. *Medical Physics*, *20*, 1033–1048.

Boykov, Y., & Kolmogorov, V. (2004). An experimental comparison of min-cut/max-flow algorithms for energy minimization in vision. *IEEE Transactions on Pattern Analysis and Machine Intelligence*, *26*(9), 1124–1137.

Boykov, Y., Veksler, O., & Zabih, R. (2001). Fast approximate energy minimization via graph cuts. *IEEE Transactions on Pattern Analysis and Machine Intelligence*, *23*(11), 1222–1239.

Boykov, Y. Y., & Jolly, M. P. (2001). Interactive graph cuts for optimal boundary & region segmentation of objects in N-D images. In *Eighth IEEE international conference on computer Vision, ICCV* (Vol. 1, pp. 105–112). Vancouver, BC, Canada.

Cao, L., Lu, Y. M., Li, C. Q., & Yang, W. (2019). Automatic segmentation of pathological glomerular basement membrane in transmission electron microscopy images with random Forest stacks. *Computational and Mathematical Methods in Medicine*, *1684218*, 1–11.

Cover, T. M., & Thomas, J. A. (1991). *Elements of information theory* (2nd ed.). John Wiley & Sons.

Daniel. (2021). Region Growing (2D/3D grayscale), MATLAB Central File Exchange. Retrieved 2021. https://www.mathworks.com/matlabcentral/fileexchange/32532-region-growing-2d-3d-grayscale

Elaziz, M. A., & Lu, S. (2019). Many-objectives multilevel thresholding image segmentation using knee evolutionary algorithm. *Expert Systems with Applications*, *125*, 305–316.

Frank, J. (2006). *Electron tomography. Methods for three-dimensional visualization of structures in the cell*. Springer.

Groom, D. J., Yu, K., Rasouli, S., Polarinakis, J., Bovik, A. C., & Ferreira, P. J. (2018). Automatic segmentation of inorganic nanoparticles in BF TEM micrographs. *Ultramicroscopy*, *194*, 25–34.

Hilali-Jaghdam, I., Ishak, A. B., Abdel-Khalek, S., & Jamal, A. (2020). Quantum and classical genetic algorithms for multilevel segmentation of medical images: A comparative study. *Computer Communications*, *162*, 83–93.

Iturrondobeitia, M., Guraya, T., Okariz, A., Srot, V., Van Aken, P. A., & Ibarretxe, J. (2017). Quantitative electron tomography of PLA/clay nanocomposites to understand the effect of the clays in the thermal stability. *Journal of Applied Polymer Science*, *134*(15), 44691.

Jing, L., Deng, D., & Yu, J. (2014). Weighting exponent selection of fuzzy C-means via Jacobian matrix. In R. Buchmann, C. V. Kifor, & J. Yu (Eds.), *Knowledge science, engineering and management, KSEM* Lecture Notes in Computer Science (Vol. 8793). Springer.

Kan, A. (2017). Machine learning applications in cell image analysis. *Immunology and Cell Biology*, *95*, 525–530.

Kotrbová, A., Štěpka, K., Maška, M., Pálenik, J. J., Ilkovics, L., Klemová, D., Kravec, M., Hubatka, F., Dave, Z., Hampl, A., Bryja, V., Matula, P., & Pospíchalová, V. (2019). TEM exosome analyzer: A computer-assisted software tool for quantitative evaluation of extracellular vesicles in transmission electron microscopy images. *Journal of Extracellular Vesicles*, *8*(1), 1560808.

Lostado, R., Villanueva Roldán, P., Fernandez Martinez, R., & Mac Donald, B. J. (2012). Design and optimization of an electromagnetic servo braking system combining finite element analysis and weight-based multi-objective genetic algorithms. *Journal of Mechanical Science and Technology*, *30*(8), 3591–3605.

Maes, F., Collignon, A., Vandermeulen, D., Marchal, G., & Suetens, P. (1997). Multimodality image registration by maximization of mutual information. *IEEE Transactions on Medical Imaging*, *16*(2), 187–198.

Magliaro, C., Callara, A. L., Vanello, N., & Ahluwalia, A. (2019). Gotta trace 'em all: A mini-review on tools and procedures for segmenting single neurons toward deciphering the structural connectome. *Frontiers in Bioengineering and Biotechnology*, *7*(222), 1–8.

Masubuchi, S., Watanabe, E., Seo, Y., Okazaki, S., Sasagawa, T., Watanabe, K., Taniguchi, T., & Machida, T. (2020). Deep-learning-based image segmentation integrated with optical microscopy for automatically searching for two-dimensional materials. *NPJ 2D Materials and Applications*, *4*(1), 1–9.

MATLAB. (2020). *Image processing toolbox 2020*. The MathWorks, Inc.

Midgley, P. A., Ward, E. P. W., Hungria, A. B., & Thomas, J. M. (2007). Nanotomography in the chemical, biological and materials sciences. *Chemical Society Reviews*, *36*(9), 1477–1494.

Mirzaei, M., & Rafsanjani, H. K. (2017). An automatic algorithm for determination of the nanoparticles from TEM images using circular hough transform. *Micron*, *96*, 86–95.

Okariz, A., Guraya, T., Iturrondobeitia, M., & Ibarretxe, J. (2017). A parameter for the assessment of the segmentation of TEM tomography reconstructed volumes based on mutual information. *Micron*, *103*, 64–77.

Okeke, F., & Karnieli, A. (2006). Linear mixture model approach for selecting fuzzy exponent value in fuzzy c-means algorithm. *Ecological Informatics*, *1*, 117–124.

Oktay, A. B., & Gurses, A. (2019). Automatic detection, localization and segmentation of nano-particles with deep learning in microscopy images. *Micron*, *120*, 113–119.

Peng, B., & Veksler, O. (2008). Parameter selection for graph cut based image segmentation. In M. Everingham & C. Needham (Eds.), *Proceedings of the British machine conference* (pp. 16.1–16.10). BMVA Press.

Pettersen, E. F., Goddard, T. D., Huang, C. C., Couch, G. S., Greenblatt, D. M., Meng, E. C., & Ferrin, T. E. (2004). UCSF chimera - a visualization system for exploratory research and analysis. *Journal of Computational Chemistry*, *25*(13), 1605–1612.

Rueden, C. T., Schindelin, J., Hiner, M. C., Dezonia, B. E., Walter, A. E., Arena, E. T., & Eliceiti, K. W. (2017). ImageJ2: ImageJ for the next generation of scientific image data. *BMC Bioinformatics*, *18*(529), 1–26.

Salahuddin, T., & Qidwai, U. (2020). Computational methods for automated analysis of corneal nerve images: Lessons learned from retinal fundus image analysis. *Computers in Biology and Medicine*, *119*, 103666.

Sanz-García, A., Pernía-Espinoza, A. V., Fernandez-Martinez, R., & Martínez-De-Pisón-Ascacíbar, F. J. (2012). Combining genetic algorithms and the finite element method to improve steel industrial processes. *Journal of Applied Logic*, *10*(4), 298–308.

Schindelin, J., Arganda-Carreras, I., Frise, E., Kaynig, V., Longair, M., Pietzschh, T., Preibisch, S., Rueden, C., Saafeld, S., Schmid, B., Tinevez, J. Y., James, D., Hartenstein, V., Eliceiri, K., Tomancak, P., & Cardona, A. (2012). Fiji: An open-source platform for biological-image analysis. *Nature Methods*, *9*(7), 676–682.

Semechko, A. (2021). Fast fuzzy c-means image segmentation. GitHub. Retrieved 2021. https://github.com/AntonSemechko/Fast-Fuzzy-C-Means-Segmentation

Shannon, C. E., & Weaver, W. (1949). *The mathematical theory of communication* (10th ed.). University of Illinois Press.

Simon, D. (2013). *Evolutionary optimization algorithms*. John Wiley & Sons.

Volkmann, N. (2010). Methods for segmentation and interpretation of electron tomographic reconstructions. *Methods in Enzymology*, *483*, 31–46.

Xiao, X., Kim, J. J., Hong, M. P., Yang, S., & Kim, Y. S. (2020). RSM and BPNN modeling in incremental sheet forming process for AA5052 sheet:Multi-objective optimization using genetic algorithm. *Metals*, *10*, 1003.

Yu, J., Cheng, Q., & Huang, H. (2004). Analysis of the weighting exponent in the FCM. *IEEE Transactions on Systems, Man, and Cybernetics. Part B, Cybernetics*, *34*(1), 634–639.

How to cite this article: Fernandez Martinez, R., Okariz, A., Iturrondobeitia, M., & Ibarretxe, J. (2023). The determination of optimum segmentation parameters using genetic algorithms: Application to different segmentation algorithms and transmission electron microscopy tomography reconstructed volumes. *Microscopy Research and Technique*, *86*(10), 1237–1248. https://doi.org/10.1002/jemt.24318